https://doi.org/10.5194/acp-2020-192
Preprint. Discussion started: 4 May 2020

Atmospheric Chemistry and Physics Discussions

How aerosols and greenhouse gases influence the diurnal temperature range

Camilla W. Stjern[1], Bjørn H. Samset[1], Olivier Boucher[2], Trond Iversen[3], Jean-François Lamarque[4], Gunnar Myhre[1], Drew Shindell[5], Toshihiko Takemura[6]

[1]CICERO Center of International Climate Research, Oslo, Norway
[2] Institut Pierre-Simon Laplace, Sorbonne Université / CNRS, Paris, France
[3] Norwegian Meteorological Institute, Oslo, Norway
[4] NCAR/UCAR, Boulder, USA
[5] Nicholas School of the Environment, Duke University, Durham, NC, USA
[6] Kyushu University, Fukuoka, Japan

Correspondence to: Camilla W. Stjern, camilla.stjern@cicero.oslo.no

Abstract. The diurnal temperature range (DTR), or difference between the maximum and minimum temperature within one day, is one of many climate parameters that affects health, agriculture and society. Understanding how DTR evolves under global warming is therefore crucial. Since physically different drivers of climate change, such as greenhouse gases and aerosols, have distinct influences on global and regional climate, predicting the future evolution of DTR requires knowledge of the effects of individual climate forcers, as well as of the future emissions mix, in particular in high emission regions. Using global climate model simulations from the Precipitation Driver and Response Model Intercomparison Project (PDRMIP), we investigate how idealized changes in the atmospheric levels of a greenhouse gas (CO_2) and aerosols (black carbon and sulfate) influence DTR, globally and in selected regions. We find broad geographical patterns of annual mean change that are similar between climate drivers, pointing to a generalized response to global warming which is not defined by the individual forcing agents. Seasonal and regional differences, however, are substantial, which highlights the potential importance of local background conditions and feedbacks. While differences in DTR responses among drivers are minor in Europe and North America, there are distinctly different DTR responses to aerosols and greenhouse gas perturbations over India and China, where present aerosol emissions are particularly high. BC induces substantial reductions in DTR, which we attribute to strong modelled BC-induced cloud responses in these regions.

1 Introduction

As the global climate warms (Hartmann et al., 2013), changes are not only observed in the daily mean temperature, but in a variety of parameters relevant to society. One such parameter is the diurnal temperature range (DTR), which is a measure of the difference between the maximum and the minimum temperature over a given day. Variations in the magnitude of the DTR

https://doi.org/10.5194/acp-2020-192
Preprint. Discussion started: 4 May 2020


Atmospheric Chemistry and Physics Discussions

have been found to influence mortality and morbidity (Cheng et al., 2014; Kim et al., 2016; Lim et al., 2012), parasite infection and transmission (Paaijmans et al., 2010), and crop failure (Hernandez-Barrera et al., 2017; Lobell, 2007). Future changes in the DTR is therefore a potential driver of climate impacts, affecting risk assessments associated with health and agriculture and have serious consequences in vulnerable regions.

Observations show a general reduction in DTR over the twentieth century, typically mediated by a stronger increase in the daily minimum temperature (T_{min}) than in the daily maximum temperature (T_{max}) (Dai et al., 1999; Karl et al., 1993; Vose et al., 2005). This trend in DTR has been linked to anthropogenic emissions, but whether greenhouse gases or aerosols are the dominating influence, and what roles these respective climate drivers will play to future DTR changes, is not clear.

Physically, a range of geophysical processes contribute to determining the land surface DTR of a given region. Maximum temperatures are reached during daytime, due to the excess of incoming shortwave (SW, or solar) radiation. Minimum temperatures occur at night, primarily due to cooling from longwave (LW, or heat) radiation. LW cooling is however active during both daytime and night-time, and thus influences both T_{min} and T_{max}, reducing the potential DTR influence of factors affecting it. Thus, greenhouse gases such as CO_2, which have a particularly strong effect on LW radiation fluxes throughout the day (e.g., Lagouarde and Brunet, 1993), are not initially expected to have the strongest direct radiative influence on DTR. Indeed, Dai et al. (1999) showed that changes in water vapor had a relatively small effect on DTR.

Aerosols, on the other hand, primarily have climate interactions affecting the shortwave (SW) spectrum, lowering the incoming SW radiation at the surface, initially reducing the daytime T_{max} and thus reducing DTR. But in addition to the direct interactions with SW and, to a lesser extent, LW radiation, greenhouse gases and aerosols alike have a range of indirect (radiative and non-radiative) influences on climate, that can cause further changes to T_{min} and T_{max}. For instance, sulfate aerosols can interact microphysically with clouds to make them more reflective (Twomey, 1974) or increase the general cloud cover by increasing cloud lifetime (Albrecht, 1989). Cloud changes have been shown to have a strong influence on DTR, primarily by blocking SW radiation and hence reducing T_{max} (e.g., Dai et al., 1999). Increased cloud thickness or cloud cover will also affect the surface energy budget, through increasing downwelling LW radiation. This effect operates during both day and night, but at high latitudes during the polar night, when there is no incoming SW radiation and the T_{max} effect is therefore absent, an increase in T_{min} from altered LW retention can reduce the DTR. The strong SW atmospheric absorption of BC and CO_2 can cause rapid adjustments in both cloudiness and precipitation through their influence on atmospheric stability (Hansen et al., 1997; Richardson et al., 2018; Stjern et al., 2017). An increase in precipitation, for instance, may induce changes in soil moisture, which could in turn influence DTR through a reduced T_{min} due to enhanced evaporation (Zhou et al., 2007). Finally, on a longer time scale, feedback responses following a warming climate can cause changes to DTR via associated changes in cloud cover (Dai et al., 1999), atmospheric circulation changes, precipitation (Karl et al., 1993), soil moisture (Zhou et al., 2007), surface

https://doi.org/10.5194/acp-2020-192
Preprint. Discussion started: 4 May 2020


Atmospheric Chemistry and Physics Discussions

heat storage capacity (Kleidon and Renner, 2017), land use changes (Mohan and Kandya, 2015), and the turbulent fluxes of sensible and latent heat in the atmospheric boundary layer (Davy et al., 2017).

Over the coming decades, we can expect to see changes in emissions of both greenhouse gases and aerosols, resulting in a global backdrop of increased greenhouse gas induced forcing, combined with an aerosol influence that has regionally heterogeneous pattern and potentially strong trends. As an example, the global burden of aerosol loading has recently shifted from Europe to Asia (Myhre et al., 2017a), which has previously been linked to an ongoing drying of the Mediterranean region (Tang et al., 2017), and changes to the South and East Asian Monsoon circulations(Wilcox et al., 2020). However, the future balance between the different climate forcers is highly uncertain, and differs markedly between informed projections such as the Shared Socioeconomic Pathways (Lund et al., 2019; Rao et al., 2017)

Understanding the separate influence of the different climate drivers on DTR, when taking into account both direct and indirect effects and their climate feedbacks, is therefore an important prerequisite for understanding how regional DTR will evolve over the coming decades. The purpose of this work is to contribute to such an understanding, based on a sample of common, idealized experiments performed by nine coupled climate models. While model studies investigating effects of greenhouse gases and aerosols on DTR have typically used historical simulations (Lewis and Karoly, 2013; Liu et al., 2016), these simulations include trends in greenhouse gases as well as trends in both scattering and absorbing aerosols, with opposite effects on global mean temperature and, possibly, on DTR. To disentangle the role of different climate drivers to the DTR changes, model responses to idealized experiments where individual drivers are perturbed separately provide a separate line of evidence.

In the present study we compare idealized instantaneous perturbations of CO_2, BC and SO_4 in nine global climate models from the Precipitation Driver Response Model Intercomparison Project (PDRMIP) (Myhre et al., 2017b). This unique data sets allows us to investigate whether differing changes to DTR can be expected from trends in greenhouse gases, sulfate or black carbon, and can shed light on results from more comprehensive, multi-forcer simulations, such as those in the Coupled Model Intercomparison Project Phase 6 (CMIP6) (Eyring et al., 2016). While the size of the dataset precludes detailed process-level investigations of the output from each model, any significant changes found based on the median response of the model sample should represent physically robust expectations based on the geophysical understanding underlying the generation of climate models participating here (which are mostly similar to their CMIP5 configurations; Myhre et al. (2017b)).

In the next section, we give a brief overview of data and methods used in this paper. Section 3 describes the main results of this study, starting with a comparison between PDRMIP baseline DTR values to observations, to show how the specific PDRMIP models capture regional DTR. The results are summarized in Section 4.

https://doi.org/10.5194/acp-2020-192
Preprint. Discussion started: 4 May 2020


Atmospheric Chemistry and Physics Discussions

2 Methods

We utilize data from the Precipitation Driver and Response Multimodel Intercomaprison Project (PDRMIP), in which nine global climate models have performed idealized simulations of instantaneous perturbations in different climate drivers. Here, we analyze the experiments involving a doubling of CO_2 (CO2x2), a tenfold increase in black carbon (BC) (BCx10) and a fivefold increase in sulfate (SO_4) (SO4x5), see Table 1. See Figure 1 for the geographical distribution of the perturbed BC and SO_4 aerosol concentration fields. The perturbations in the experiments were designed to produce clear and robust climate signals, and the magnitude of the resulting changes are therefore larger than what can be expected from current changes in climate drivers. Moreover, near-equilibrium changes from these abrupt perturbations will likely yield different responses to the gradual build-up (of e.g. CO_2) seen in the real word. Note that for the aerosol perturbations, some models perturbed concentrations while others perturbed emissions. This leads to some additional inter-model differences in forcing and response patterns, but has previously been shown not to be a major determining factor for PDRMIP results based on global perturbations (Stjern et al., 2017).

The perturbation experiments are performed and compared relative to baseline simulations representing present-day conditions and using emissions/concentration and solar constant values for year 2000 (except HadGEM2, which used a preindustrial baseline). See Table 1 and (Myhre et al., 2017b; Samset et al., 2016; Stjern et al., 2017) for details and a list of models. All the simulations were 100 years long. Data for the simulation years 51-100 were used in the analyses, and changes were defined as the average of these years for a perturbed simulation minus the corresponding average for the baseline simulation.

DTR was calculated based on daily minimum temperature (T_{min}) and maximum temperature (T_{max}) values and averaged into monthly and seasonal means. To determine whether a given DTR change is significantly different from zero, regional mean monthly mean DTR values over a 50-year period, for perturbed versus baseline climates, were tested for each model and experiment using Student's t-test ($p<0.05$).

We have chosen to limit our analysis to land regions and will present results for all land (LND), the United States region (USA), central Europe (EUR), India (IND), eastern China (CHI), and the Arctic (ARC). Regions are chosen partly to present results for the world's most populated regions, and partly where previous findings point to large historical changes in DTR and where changes in the future are of particular interest.

3 Results and Discussion

This section presents the global, annual land mean modelled DTR changes in response to the PDRMIP perturbations, as well as regionally and seasonally resolved results. However, as earlier work has demonstrated a tendency in CMIP5-generation models to underestimate DTR relative to observations, with a bias that differs strongly between models and regions (Sillmann et al., 2013), we start our analysis by comparing the PDRMIP baseline DTR values to surface temperature observations.

https://doi.org/10.5194/acp-2020-192
Preprint. Discussion started: 4 May 2020


Atmospheric Chemistry and Physics Discussions

3.1 Comparison to observations

Figure 2 compares PDRMIP DTR, T_{min} and T_{max} for the baseline (year 2000) simulations to gridded observational data from the Climate Research Unit (CRU) TS v. 4.03 (Harris et al., 2014) averaged over years 1991-2010. The observational data set as well as all models are regionally averaged at their native grid resolution. While the multi-model median land annual mean DTR of 10.8 K is smaller than the CRU value of 11.5 K, individual model values have a standard deviation of 2.56 and range from 8.2 to 15.8 K (Fig. 2a). HadGEM3, NCAR-CESM-CAM4 and CanESM2 have consistently high DTR values, while GISS-E2-R, NorESM1-M and NCAR-CESM-CAM5 have the lowest values. (HadGEM2 has been omitted here, since it used a preindustrial baseline.) As the single-realization simulations performed here will be sensitive to the timing of internal variability among model simulations, this will likely cause some of the inter-model differences. However, the model spread is not sensitive to the exact time period used. As a crude test, we picked out 20-year periods from the 50 years of the baseline simulations, moving 5 years at a time (giving 7 20-year periods within the 50 years of data), and found that inter-model standard deviations of DTR for these periods ranged between 2.555 and 2.564. While this indicates that model differences are more likely related to actual differences in model formulations and parametrizations, we note that internal variations in regional clouds and precipitation – which strongly influence DTR – can affect trends over periods up to 60 years (Deser et al., 2012), making it difficult to compare changes in DTR both among models and between models and observations.

Although the geographical DTR pattern is similar between the model median and observations (Fig. 2b), notable differences can also be seen. See for instance western North America, where the modelled DTR is substantially lower than the observed. One known issue in atmospheric models is the representation of the atmospheric boundary layer at high latitudes (e.g., Steeneveld, 2014), where wintertime minimum temperatures are often determined by a very thin and stable boundary layer. Figure 2a shows that minimum temperatures for most of the models are higher than observations in the northernmost regions investigated here, notably Europe and North America, which explains the underestimated DTR. In the Arctic, however, there is lower model agreement also in estimates of T_{min}, with about half the models showing a warm bias, and the other half a cold bias of T_{min}. In India and China, on the other hand, T_{min} tends to be too cold, although this is balanced by T_{max} also having a cold bias in many of the models.

Inter-model spread is in all regions larger for T_{max} than T_{min}, and for T_{max} there is also more model disagreement as to the sign of the bias relative to observations. Note, for instance, that for T_{max} in USA, four models overestimate while four models underestimate.

Overall, the PDRMIP models perform similarly to CMIP5 models in general (Sillmann et al., 2013), with a general underestimation of DTR, but with large differences between models as well as between regions. Although no direct comparison between historical DTR changes and the idealized simulations in this study will be made, the caveats noted above should be kept in mind in interpretations of the analyses below.

https://doi.org/10.5194/acp-2020-192
Preprint. Discussion started: 4 May 2020


Atmospheric Chemistry and Physics Discussions

3.2 DTR change in response to different forcing mechanisms

Figure 3 shows how the three drivers (CO_2, BC and SO_4) influence the DTR for the annual mean (large upper panels) and for the different seasons (small panels). To make the comparison easier between the drivers, the DTR change is divided by the global, annual mean temperature change for each driver and model, and thus shows how DTR will change for a 1°C surface warming due to perturbations in the given climate driver. Model median global temperature change and model spread for the three drivers are 2.6 [1.5 to 3.7] K (CO2x2), 0.7 [0.2 to 1.7] K (BCx10) and -1.65 [-0.9 to -6.6] K (SO4x), respectively (see Samset et al. (2016) for core analysis of all PDRMIP experiments and models). For SO_4, which cools the climate, this normalization switches the sign of the change and shows in principle the result of a reduced SO_4 level, as opposed to the other drivers. As the tenfold increase in BC, particularly for some of the models, has a weak impact on global temperatures (Stjern et al., 2017), normalization by these small numbers leads to particularly large normalized DTR changes for the BCx10 experiment. However, as seen by comparing absolute DTR changes for BCx10 in Fig. S2 to those of CO2x2 and SO4x5 (Figs. S1, and S3), the absolute DTR change for BCx10 is also large in itself: an annual mean model median DTR change of -0.03 K (compared to -0.05 K for CO2x2) is substantial given than the doubling of CO_2 causes a four times stronger response in the global mean temperature.

The geographical patterns of annual mean DTR change are relatively similar between the drivers. All drivers show reduced DTR at high latitudes (see the Arctic), increased DTR in mid-latitudes (see, e.g. USA and central/southern Europe), increased DTR over the Amazon and southern Africa, and reduced DTR over northern/central Africa. The small panels in Fig. 3 shows that the largest seasonal differences in DTR responses are found between summer (JJA) and winter (DJF) for all driver. In the next sections we will therefore take a closer look at these two seasons.

3.2.1 Wintertime DTR responses

All three climate drivers induce a strong reduction in DTR over northern high and mid latitudes in winter (Fig. 3). Figure 4 shows regional, multi-model mean DTR changes for each season and driver. Colored bars indicate high inter-model consistency, defined as cases where 80% of models with data have changes of the same sign. In wintertime there is a robust (colored bars for all drivers) reduction in DTR over Europe and the Arctic. Numbers below the bars indicate for how many of the nine models these changes are statistically significant, and the number is high for both these regions. A similar reduction is seen over USA, but here there is lower model agreement on the BC-induced DTR reduction.

As shown in Fig. 5, the wintertime DTR reduction in these northern mid and high latitudes is driven by an increase in T_{min} that is stronger than the increase in T_{max}. Previous studies have shown that while the general global warming, instigated for instance by increased greenhouse gases, can be expected to increase both T_{min} and T_{max}, an increase in cloud cover can substantially dampen the increase in T_{max} (e.g., Dai et al., 1999), resulting in a DTR reduction. We therefore take a closer look at how greenhouse gases and aerosols influence the cloud cover in these regions.

https://doi.org/10.5194/acp-2020-192
Preprint. Discussion started: 4 May 2020


Atmospheric Chemistry and Physics Discussions

Tables S1-S6 show correlation coefficients between changes in DTR and changes in related variables (cloud cover, latent and sensible heat flux, clear-sky and all-sky downwelling SW radiation and all-sky downwelling LW radiation). Here we see that there are statistically significant negative correlations between cloud amount changes and changes in DTR for all these regions, confirming that more clouds are associated with lower DTR. Figure 6 and Table S1 shows cloud cover changes for winter and summer, for the three drivers.

For CO2x2 and SO4x5, we do find a slight increase in cloud cover in the USA, EUR and ARC regions, which would contribute to the pattern of T_{max} and T_{min} changes seen in Fig. 5. For BCx10, however, we find a reduction in clouds over Europe but increases over USA and the Arctic. Wintertime changes in Tmin and Tmax for both aerosol experiments for Europe show very strong differences and thus strong DTR change (Fig. 5 and Fig. 4). Table S3 shows statistically significant correlations between DTR change and the change in clear-sky downwelling radiation for these two experiments, and for BCx10 the reduction in this variable is particularly strong (Table S8) – likely enough to dampen T_{max} in spite of the slight reduction in cloud cover.

In the Arctic region (recall that our regional averages only land, not ocean, areas in this study), the lack of incoming solar radiation in winter means that the increase in T_{max} will be dampened to a lesser degree, and the difference between the changes in T_{min} and T_{max} will be smaller. This can be seen in Fig. 5, where the wintertime slopes between T_{min} and T_{max} are much weaker for the ARC region than, e.g. for EUR, manifesting in a weaker DTR change (Fig. 4).

All in all, a prominent wintertime feature in the EUR, USA and ARC regions is a consistency between drivers in terms of changes to T_{min} and T_{max}, ultimately all causing a reduction in DTR. We see, however, that although greenhouse gases and aerosols influence DTR in the same manner, the underlying processes differ between drivers.

3.2.2 Summertime DTR responses

The reduced wintertime DTR in mid-latitudes is contrasted by a strong summertime increase. Europe stands out as the region with the best inter-model agreement (Fig. 4; all bars are colored), with a clear summertime DTR increase for all three drivers that stems from a much stronger increase in T_{max} than in T_{min} (Fig. 7). The same can be seen for USA, albeit with less agreement between models for the CO_2 response. In both these regions, all three drivers induce substantial reductions in summertime cloud cover (Fig. 6), driving the strong increase in T_{max}. The link between DTR and cloud changes is supported by strong and statistically significant correlations between the two (Tables S2 and S3), with corresponding correlations to sensible heat flux and the amount of downwelling SW radiation, which we expect to increase as the cloud cover diminishes. A reduction in summertime precipitation in this region (not shown) contributes to the T_{max} enhancement as a drier climate tends to involve less clouds and a drier surface with less evaporation. These are conditions that lower the night-time temperatures and increase daytime temperatures, thus contributing to increased DTR. It is well know from observations that the last decades have seen a marked drying of Europe in the summer (Manabe and Wetherald, 1987; Rowell and Jones, 2006; Vautard et al., 2014; Leduc et al., 2019), potentially as a result of an expanding Hadley cell (Lau and Kim, 2015) or due to weaker lapse-rate changes over the Mediterranean region than over northern Europe (Brogli et al., 2019).

https://doi.org/10.5194/acp-2020-192
Preprint. Discussion started: 4 May 2020


Atmospheric Chemistry and Physics Discussions

Based on observations, Makowski et al. (2008) found a strong increase in European DTR in the period of strong SO_2 mitigations in the region, and suggested a causal relationship. Although natural variability and other forcing mechanisms have likely contributed to these trends, the increase in DTR over Europe seen in the SO4x5 experiment (recall the normalization by temperature change, meaning that this experiment corresponds to a SO_4 reduction) is consistent with the findings of Makowski et al. (2008). However, as our SO_4 perturbation experiment causes DTR increases that are comparable with what is caused by perturbations of BC and CO_2, it seems that the DTR change in Europe is not a driver specific response solely linked to the trends in aerosols, but rather part of a larger response to the general warming of the climate and the resulting large-scale circulation changes.

In the Arctic region, we find differences in summertime DTR response between the drivers. CO_2 causes a stronger Arctic increase in T_{max} than in T_{min} and thus an increased DTR for all models, while BC for most models causes a stronger increase in T_{min} and thus DTR reduction (Fig. 7). The reason is that CO_2 induces a reduction in the summertime Arctic cloud cover, consistent with the increase in T_{max}, while BC enhances the cloud cover, thus hindering the strong T_{max} increase. Indeed, calculating SW and LW cloud radiative effects (CRE, Fig. 8) as the difference between clear-sky and all-sky top-of-atmosphere radiative fluxes (see, e.g., Dessler and Zelinka, 2015), we see a strong summertime SW cloud radiative cooling over Arctic land masses for BCx10 (-7.0 $Wm^{-2}K^{-1}$) (much stronger than the LW CRE effect, thus indicating that the change is primarily to low clouds), contrasting a small positive CRE (+0.2 $Wm^{-2}K^{-1}$) for CO2x2.

We have now shown that, in general, responses to greenhouse gases and aerosols have similar effects on DTR in northern mid and high latitudes. Next, we move on to the high aerosol-emission regions of India and China, to illustrate that in regions of high aerosol emissions, the slight differences in how greenhouse gases and aerosols influence DTR will result in much more prominent differences in DTR change between the drivers.

3.2.3 Driver-specific DTR changes over India and China

Near-term changes in aerosols over India and China, as envisioned in the Shared Socioeconomic Pathways (Rao et al. 2017), project either reduced concentrations of BC and SO_4 in both regions, increased concentrations of BC and SO_4 in India but reductions in China, or increased BC over both regions but a dipole pattern of increase over India but decrease over China (Samset et al., 2019). Given this uncertainty in future emission trends, understanding the individual responses of DTR to these two aerosol species is of high interest. In our simulations, BC causes strong DTR changes in all regions (Fig. 4), but particularly in India and China where present-day aerosol concentrations (and thus the magnitude of the perturbations) are high (Fig. 1). There is a high level of agreement between models on the sign of the DTR changes, which is striking, as BC-induced climate changes have been shown repeatedly to be associated with higher levels of model disagreement than changes driven by CO_2 and SO_4 (Richardson et al., 2018; Samset et al., 2016). Contrasting the strong inter-driver consistency in DTR changes in northern mid latitudes, we find the DTR-response of BC to differ more from the other drivers in India and China, where strongly negative BC-induced DTR changes stand out from the other drivers in both seasons.

https://doi.org/10.5194/acp-2020-192
Preprint. Discussion started: 4 May 2020


Atmospheric Chemistry and Physics Discussions

Changes in aerosol concentrations have been suggested as a cause of the DTR changes in China (Dai et al., 1999; Liu et al., 2004). Here, we find relatively weak correlations between the DTR changes and changes in the BC burden (0.26 and 0.38 in summer in India in DJF and JJA, respectively, and 0.12 and 0.29 in China). Still, correlations between DTR changes and changes in downwelling clear-sky SW radiation (Tables S4 and S5) are strong and significant, at least in India. Interestingly, for both BCx10 and SO4x5, the aerosol perturbations are stronger in China than in India (Fig. 1), and Table S8 shows that the magnitude of the change in downwelling clear-sky SW radiation is also strongest in China. Still, the link between these changes and DTR are strongest in India. We find that in the BASE simulations, India tends towards a slightly drier climate with less precipitation, less surface evaporation, less cloud cover and a stronger sensible heat flux than China (not shown) – properties typically associated with warmer maximum and colder minimum temperatures. India therefore has a higher DTR to begin with (Fig. 2a), and thus a larger potential for change in the DTR.

In winter, the only substantial DTR changes can be seen for BCx10 in the China region, for which the increase in T_{max} is very weak (Fig. 5), likely due to a simulated increase in clouds for this experiment (Fig. 6). The same can be seen in summer, for which DTR reduction in China due to BC also goes down and cloud levels up. In India, most models agree that the increase in summertime T_{min} is stronger than in T_{max}, causing reduced DTR for all three drivers. However, this effect is substantially stronger for BC than for CO_2 and SO_4. Figure 7 shows that the extremely strong DTR reduction for BCx10 over India in summer occurs because T_{min} is slightly enhanced while T_{max} is actually reduced. The reduction in T_{max} is seen for all models but IPSL-CM5A, which is the only model for which cloud cover decreases over India in this season. For the other models, the summertime cloud cover increase from the BCx10 experiment, as clearly seen in Fig. 6, is substantial over India. In particular, there is a strong reduction in the SW CRE over India (Fig. 8), likely responsible for the reduction in summertime T_{max}. Oppositely, the increase in summertime T_{min} (nighttime temperatures are influenced only by the LW spectrum) is enhanced by the positive change in LW CRE over India. In fact, regions which have both a negative change in the SW CRE and a positive change in the LW CRE can be recognized as the regions with the strongest reductions in DTR in the BCx10 JJA map of Fig. 3 (most importantly India and Central Africa).

The strong link between cloud and DTR changes is confirmed by significant negative correlations between DTR and cloud cover in the India and China regions (Tables S4 and S5), strongest in the summer. A previous analysis of the PDRMIP BCx10 experiment by Stjern et al. (2017) found that the BC-induced cloud amount increases in these regions were strongly driven by rapid cloud adjustments (including the so-called semi-direct effect), but were also a part of the longer-term response to increased global surface temperatures. The cloud increases were stronger in India than in China, particularly for low clouds, which have the strongest influence on T_{max}.

All in all, while we do see that aerosol-radiation interactions have likely contributed to the regions' DTR changes (through reduction in downwelling SW radiation and thus surface heating), the strongest link again seems to be clouds. Greenhouse gases and aerosols cause distinctly different responses in DTR in the regions – not primarily through their direct radiative

https://doi.org/10.5194/acp-2020-192
Preprint. Discussion started: 4 May 2020


Atmospheric Chemistry and Physics Discussions

effect, but via their specific influence on cloud cover. As cloud responses to the strong BC perturbations are so substantial, especially in India, the BC response in DTR stands out here.

Given the strong role of clouds in the DTR response, estimates of DTR change will be sensitive to the way that specific climate forcers influence clouds in different climate models, and to their baseline cloud representations. Model responses to CO_2 perturbations have been shown to vary greatly between individual models, and responses to aerosols have even larger uncertainties, partly due to additional variations in parametrizations of indirect and semidirect effects. For instance, both a previous PDRMIP analysis of the BCx10 experiment (Stjern et al., 2017), and an idealized single-model study (Samset and Myhre 2015), indicate that increased BC concentrations lead to rapid adjustments in the form of increased fractions of low clouds and reduced fractions of high clouds over large areas of the globe, with a global mean cooling effect. In a recent study, however, Allen et al. (2019) find indications that the heating rate induced by BC is less "top heavy" than what is calculated in many climate models (i.e., the vertical profile of short wave heating rates is too uniform), and if the overestimated upper-level cloud response is corrected for, it could instead produce rapid adjustments that warm the climate, on average. These nuances are relevant to the accuracy of DTR simulations as a BC-induced reduction in high clouds will cause LW cooling and likely lower T_{min}, while increased low clouds will cause SW cooling and also lower T_{max}, with effects on the DTR depending on which is influenced the most. If, on the other hand, BC causes strong reductions in low clouds (increases T_{max}) and also weak reductions in high clouds (reduces T_{min} slightly), this will contribute to an increase in DTR. More research is needed on modelled cloud responses and the vertical distribution on BC, but we note that both Stjern et al. (2017) and Allen et al. (2019) find that in the high-emission regions of India, China and North/Central Africa, the rapid adjustments produce an increase throughout all cloud layers with a total cooling effect (compare to Fig. 8, where the SW CRE is stronger than the LW CRE in these regions) and likely with similar effects on the DTR.

4 Summary and Conclusion

We have analyzed a multi-model set of idealized simulations to investigate how changes to the atmospheric levels of CO_2, BC and SO_4 influence the diurnal temperature range, through alterations of global mean surface temperature, cloud amounts and other climate parameters. For northern mid-latitude regions, we find DTR changes that are broadly similar between drivers. The cause of the DTR change, as apparent from patterns of T_{min} and T_{max} changes, is not always the same for all drivers. However, the resulting change is consistently an increase in DTR in summer, in EUR, USA and ARC, and a decrease in winter. This similarity may partly be the result of general atmospheric response to changes in surface temperature, rather than the distinct processes through which the drivers operate. Thus, while the strong DTR reductions over Europe have been linked to the massive mitigation effort of SO_4 over the past decades, our similar responses of SO_4 perturbations to perturbations of CO_2 and BC indicate that this is not necessarily an aerosol-specific response.

https://doi.org/10.5194/acp-2020-192
Preprint. Discussion started: 4 May 2020


Atmospheric Chemistry and Physics Discussions

Over India and China there is less agreement between drivers, with BC causing a strong DTR reduction in both regions in all seasons. The inter-model spread is large, but all models agree on the sign of this change. Although the strong short-wave atmospheric absorption induced by BC particles is predominantly active in daytime, thus impacting the maximum (daytime) temperature more than the minimum (nighttime) temperature, we find that the direct aerosol effect is likely not the leading cause of the DTR response. Rather, it is the strong cloud response to BC in these regions, shown in previous studies to result from aerosol-induced changes to atmospheric stability and relative humidity, that drive the response in DTR. All models have stronger correlations to cloud related variables than to clear-sky radiative fluxes or changes in BC burden. Hence, the very high BC concentrations in this region have a strong influence on clouds, and thus on DTR.

Although these high-emission regions seem to have driver-specific responses in the DTR, in some seasons, e.g. during autumn over India, CO_2 and SO_4 produce DTR-changes of the same sign as BC, again indicating the existence of an underlying, driver-independent DTR response tied to the general warming of the climate. This supports the work of Vinnarasi et al. (2017), who stressed that observed DTR changes over India are a result of both local and global factors working in tandem.

Disentangling the role of aerosols and greenhouse gases to DTR changes is a crucial step towards prediction of future changes in regional DTR. As noted by Vinnarasi et al. (2017), detailed analyses of DTR over regions such as India and East Asia is crucial given the associated risks, which are aggravated by agriculture-dependent economies and dense populations. Moreover, in these regions, future trends in aerosol emissions are likely to be strong but are also highly uncertain. Understanding how greenhouse gases, absorbing aerosols and scattering aerosols individually influence the DTR may help these regions prepare for future changes.

Data availability

The PDRMIP model output is publicly available; for data access, visit http://www.cicero.uio.no/en/PDRMIP/PDRMIP-data-access.

Author contribution

CWS, BHS and GM designed the analyses, and CWS carried them out. BHS, OB, JFL and TT performed model simulations. CWS prepared the manuscript with contributions from all co-authors.

Competing interests

The authors declare that they have no conflict of interest.

Acknowledgements

PDRMIP is partly funded through the Norwegian Research Council project NAPEX (project number 229778). CWS and BHS were funded through the Norwegian Research Council project NetBC (project number 244141). T. T. was supported by JSPS KAKENHI Grant Number JP19H05669. O.B. acknowledges HPC resources from TGCC under the gencmip6 allocation provided by GENCI (Grand Equipement National de Calcul Intensif).

https://doi.org/10.5194/acp-2020-192
Preprint. Discussion started: 4 May 2020

Atmospheric Chemistry and Physics Discussions

345

References

Albrecht, B. A.: Aerosols, Cloud Microphysics, and Fractional Cloudiness, Science, 245, 1227-1230, 10.1126/science.245.4923.1227, 1989.

Allen, R. J., Amiri-Farahani, A., Lamarque, J.-F., Smith, C., Shindell, D., Hassan, T., and Chung, C. E.: Observationally constrained aerosol–cloud semi-direct effects, npj Climate and Atmospheric Science, 2, 16, 10.1038/s41612-019-0073-9, 2019.

Brogli, R., Kröner, N., Sørland, S. L., Lüthi, D., and Schär, C.: The Role of Hadley Circulation and Lapse-Rate Changes for the Future European Summer Climate, Journal of Climate, 32, 385-404, 10.1175/jcli-d-18-0431.1, 2019.

Cheng, J., Xu, Z., Zhu, R., Wang, X., Jin, L., Song, J., and Su, H.: Impact of diurnal temperature range on human health: a systematic review, International Journal of Biometeorology, 58, 2011-2024, 10.1007/s00484-014-0797-5, 2014.

Dai, A., Trenberth, K. E., and Karl, T. R.: Effects of Clouds, Soil Moisture, Precipitation, and Water Vapor on Diurnal Temperature Range, Journal of Climate, 12, 2451-2473, 10.1175/1520-0442(1999)012<2451:Eocsmp>2.0.Co;2, 1999.

Davy, R., Esau, I., Chernokulsky, A., Outten, S., and Zilitinkevich, S.: Diurnal asymmetry to the observed global warming, International Journal of Climatology, 37, 79-93, 10.1002/joc.4688, 2017.

Deser, C., Knutti, R., Solomon, S., and Phillips, A. S.: Communication of the role of natural variability in future North American climate, Nature Climate Change, 2, 775-779, 10.1038/nclimate1562, 2012.

Dessler, A. E., and Zelinka, M. D.: CLIMATE AND CLIMATE CHANGE | Climate Feedbacks, in: Encyclopedia of Atmospheric Sciences (Second Edition), edited by: North, G. R., Pyle, J., and Zhang, F., Academic Press, Oxford, 18-25, 2015.

Eyring, V., Bony, S., Meehl, G. A., Senior, C. A., Stevens, B., Stouffer, R. J., and Taylor, K. E.: Overview of the Coupled Model Intercomparison Project Phase 6 (CMIP6) experimental design and organization, Geosci. Model Dev., 9, 1937-1958, 10.5194/gmd-9-1937-2016, 2016.

Hansen, J., Sato, M., and Ruedy, R.: Radiative forcing and climate response, Journal of Geophysical Research: Atmospheres, 102, 6831-6864, 10.1029/96jd03436, 1997.

Harris, I., Jones, P. D., Osborn, T. J., and Lister, D. H.: Updated high-resolution grids of monthly climatic observations – the CRU TS3.10 Dataset, International Journal of Climatology, 34, 623-642, 10.1002/joc.3711, 2014.

Hartmann, D. L., Klein Tank, A. M. G., Rusticucci, M., Alexander, L. V., Brönnimann, S., Charabi, Y., Dentener, F. J., Dlugokencky, E. J., Easterling, D. R., Kaplan, A., Soden, B. J., Thorne, P. W., Wild, M., and Zhai, P. M.: Observations: Atmosphere and Surface, in: Climate Change 2013: The Physical Science Basis. Contribution of Working Group I to the Fifth Assessment Report of the Intergovernmental Panel on Climate Change, edited by: Stocker, T. F., Qin, D., Plattner, G.-K., Tignor, M., Allen, S. K., Boschung, J., Nauels, A., Xia, Y., Bex, V., and Midgley, P. M., Cambridge University Press, Cambridge, United Kingdom and New York, NY, USA, 159–254, 2013.

Hernandez-Barrera, S., Rodriguez-Puebla, C., and Challinor, A. J.: Effects of diurnal temperature range and drought on wheat yield in Spain, Theoretical and Applied Climatology, 129, 503-519, 10.1007/s00704-016-1779-9, 2017.

Karl, T. R., Jones, P. D., Knight, R. W., Kukla, G., Plummer, N., Razuvayev, V., Gallo, K. P., Lindseay, J., Charlson, R. J., and Peterson, T. C.: A New Perspective on Recent Global Warming: Asymmetric Trends of Daily Maximum and Minimum Temperature, Bulletin of the American Meteorological Society, 74, 1007-1024, 10.1175/1520-0477(1993)074<1007:Anporg>2.0.Co;2, 1993.

Kim, J., Shin, J., Lim, Y.-H., Honda, Y., Hashizume, M., Guo, Y. L., Kan, H., Yi, S., and Kim, H.: Comprehensive approach to understand the association between diurnal temperature range and mortality in East Asia, Science of The Total Environment, 539, 313-321, https://doi.org/10.1016/j.scitotenv.2015.08.134, 2016.

Kleidon, A., and Renner, M.: An explanation for the different climate sensitivities of land and ocean surfaces based on the diurnal cycle, Earth Syst. Dynam., 8, 849-864, 10.5194/esd-8-849-2017, 2017.

Lagouarde, J. P., and Brunet, Y.: A simple model for estimating the daily upward longwave surface radiation flux from NOAA-AVHRR data, International Journal of Remote Sensing, 14, 907-925, 10.1080/01431169308904386, 1993.

https://doi.org/10.5194/acp-2020-192
Preprint. Discussion started: 4 May 2020

Atmospheric Chemistry and Physics Discussions

Lau, W. K. M., and Kim, K.-M.: Robust Hadley Circulation changes and increasing global dryness due to CO₂ warming from CMIP5 model projections, Proceedings of the National Academy of Sciences, 112, 3630-3635, 10.1073/pnas.1418682112, 2015.

Leduc, M., Mailhot, A., Frigon, A., Martel, J.-L., Ludwig, R., Brietzke, G. B., Giguère, M., Brissette, F., Turcotte, R., Braun, M., and Scinocca, J.: The ClimEx Project: A 50-Member Ensemble of Climate Change Projections at 12-km Resolution over Europe and Northeastern North America with the Canadian Regional Climate Model (CRCM5), Journal of Applied Meteorology and Climatology, 58, 663-693, 10.1175/jamc-d-18-0021.1, 2019.

Lewis, S. C., and Karoly, D. J.: Evaluation of Historical Diurnal Temperature Range Trends in CMIP5 Models, Journal of Climate, 26, 9077-9089, 10.1175/jcli-d-13-00032.1, 2013.

Lim, Y.-H., Hong, Y.-C., and Kim, H.: Effects of diurnal temperature range on cardiovascular and respiratory hospital admissions in Korea, Science of The Total Environment, 417-418, 55-60, https://doi.org/10.1016/j.scitotenv.2011.12.048, 2012.

Liu, B., Xu, M., Henderson, M., Qi, Y., and Li, Y.: Taking China's Temperature: Daily Range, Warming Trends, and Regional Variations, 1955–2000, Journal of Climate, 17, 4453-4462, 10.1175/3230.1, 2004.

Liu, L., Li, Z., Yang, X., Gong, H., Li, C., and Xiong, A.: The long-term trend in the diurnal temperature range over Asia and its natural and anthropogenic causes, Journal of Geophysical Research: Atmospheres, 121, 3519-3533, 10.1002/2015jd024549, 2016.

Lobell, D. B.: Changes in diurnal temperature range and national cereal yields, Agricultural and Forest Meteorology, 145, 229-238, https://doi.org/10.1016/j.agrformet.2007.05.002, 2007.

Lund, M. T., Myhre, G., and Samset, B. H.: Anthropogenic aerosol forcing under the Shared Socioeconomic Pathways, Atmos. Chem. Phys., 19, 13827-13839, 10.5194/acp-19-13827-2019, 2019.

Makowski, K., Wild, M., and Ohmura, A.: Diurnal temperature range over Europe between 1950 and 2005, Atmos. Chem. Phys., 8, 6483-6498, 10.5194/acp-8-6483-2008, 2008.

Manabe, S., and Wetherald, R. T.: Large-Scale Changes of Soil Wetness Induced by an Increase in Atmospheric Carbon Dioxide, Journal of the Atmospheric Sciences, 44, 1211-1236, 10.1175/1520-0469(1987)044<1211:lscosw>2.0.co;2, 1987.

Mohan, M., and Kandya, A.: Impact of urbanization and land-use/land-cover change on diurnal temperature range: A case study of tropical urban airshed of India using remote sensing data, Science of The Total Environment, 506-507, 453-465, https://doi.org/10.1016/j.scitotenv.2014.11.006, 2015.

Myhre, G., Samset, B. H., Schulz, M., Balkanski, Y., Bauer, S., Berntsen, T. K., Bian, H., Bellouin, N., Chin, M., Diehl, T., Easter, R. C., Feichter, J., Ghan, S. J., Hauglustaine, D., Iversen, T., Kinne, S., Kirkevåg, A., Lamarque, J. F., Lin, G., Liu, X., Lund, M. T., Luo, G., Ma, X., van Noije, T., Penner, J. E., Rasch, P. J., Ruiz, A., Seland, Ø., Skeie, R. B., Stier, P., Takemura, T., Tsigaridis, K., Wang, P., Wang, Z., Xu, L., Yu, H., Yu, F., Yoon, J. H., Zhang, K., Zhang, H., and Zhou, C.: Radiative forcing of the direct aerosol effect from AeroCom Phase II simulations, Atmos. Chem. Phys., 13, 1853-1877, 10.5194/acp-13-1853-2013, 2013.

Myhre, G., Aas, W., Cherian, R., Collins, W., Faluvegi, G., Flanner, M., Forster, P., Hodnebrog, Ø., Klimont, Z., Lund, M. T., Mülmenstädt, J., Lund Myhre, C., Olivié, D., Prather, M., Quaas, J., Samset, B. H., Schnell, J. L., Schulz, M., Shindell, D., Skeie, R. B., Takemura, T., and Tsyro, S.: Multi-model simulations of aerosol and ozone radiative forcing due to anthropogenic emission changes during the period 1990–2015, Atmos. Chem. Phys., 17, 2709-2720, 10.5194/acp-17-2709-2017, 2017a.

Myhre, G., Forster, P. M., Samset, B. H., Hodnebrog, Ø., Sillmann, J., Aalbergsjø, S. G., Andrews, T., Boucher, O., Faluvegi, G., Fläschner, D., Kasoar, M., Kharin, V., Kirkevåg, A., Lamarque, J.-F., Olivié, D., Richardson, T., Shindell, D., Shine, K. P., Stjern, C. W., Takemura, T., Voulgarakis, A., and Zwiers, F.: PDRMIP: A Precipitation Driver and Response Model Intercomparison Project, Protocol and preliminary results, Bulletin of the American Meteorological Society, 98, 1185-1198, doi: 10.1175/BAMS-D-16-0019.1, 2017b.

Paaijmans, K. P., Blanford, S., Bell, A. S., Blanford, J. I., Read, A. F., and Thomas, M. B.: Influence of climate on malaria transmission depends on daily temperature variation, Proceedings of the National Academy of Sciences, 107, 15135-15139, 10.1073/pnas.1006422107, 2010.

Rao, S., Klimont, Z., Smith, S. J., Van Dingenen, R., Dentener, F., Bouwman, L., Riahi, K., Amann, M., Bodirsky, B. L., van Vuuren, D. P., Aleluia Reis, L., Calvin, K., Drouet, L., Fricko, O., Fujimori, S., Gernaat, D., Havlik, P., Harmsen, M., Hasegawa, T., Heyes, C., Hilaire, J., Luderer, G., Masui, T., Stehfest, E., Strefler, J., van der Sluis, S., and Tavoni, M.: Future

air pollution in the Shared Socio-economic Pathways, Global Environmental Change, 42, 346-358, https://doi.org/10.1016/j.gloenvcha.2016.05.012, 2017.

Richardson, T. B., Forster, P. M., Andrews, T., Boucher, O., Faluvegi, G., Fläschner, D., Hodnebrog, Ø., Kasoar, M., Kirkevåg, A., Lamarque, J.-F., Myhre, G., Olivié, D., Samset, B. H., Shawki, D., Shindell, D., Takemura, T., and Voulgarakis, A.: Drivers of Precipitation Change: An Energetic Understanding, Journal of Climate, 31, 9641-9657, 10.1175/jcli-d-17-0240.1, 2018.

Rowell, D. P., and Jones, R. G.: Causes and uncertainty of future summer drying over Europe, Climate Dynamics, 27, 281-299, 10.1007/s00382-006-0125-9, 2006.

Samset, B. H., Myhre, G., Schulz, M., Balkanski, Y., Bauer, S., Berntsen, T., Bian, H., Bellouin, N., Diehl, T., Easter, R. C., Ghan, S. J., Iversen, T., Kinne, S., Kirkevåg, A., Lamarque, J. F., Lin, G., Liu, X., Penner, J. E., Seland, Ø., Skeie, R. B., Stier, P., Takemura, T., Tsigaridis, K., and Zhang, K.: Black carbon vertical profiles strongly affect its radiative forcing uncertainty, Atmos. Chem. Phys., 13, 2423-2434, 10.5194/acp-13-2423-2013, 2013.

Samset, B. H., Myhre, G., Forster, P. M., Hodnebrog, Ø., Andrews, T., Faluvegi, G., Fläschner, D., Kasoar, M., Kharin, V., Kirkevåg, A., Lamarque, J. F., Olivié, D., Richardson, T., Shindell, D., Shine, K. P., Takemura, T., and Voulgarakis, A.: Fast and slow precipitation responses to individual climate forcers: A PDRMIP multimodel study, Geophysical Research Letters, 43, 2782-2791, 10.1002/2016GL068064, 2016.

Samset, B. H., Lund, M. T., Bollasina, M., Myhre, G., and Wilcox, L.: Emerging Asian aerosol patterns, Nature Geoscience, 12, 582-584, 10.1038/s41561-019-0424-5, 2019.

Sillmann, J., Kharin, V. V., Zhang, X., Zwiers, F. W., and Bronaugh, D.: Climate extremes indices in the CMIP5 multimodel ensemble: Part 1. Model evaluation in the present climate, Journal of Geophysical Research: Atmospheres, 118, 1716-1733, doi:10.1002/jgrd.50203, 2013.

Steeneveld, G.-J.: Current challenges in understanding and forecasting stable boundary layers over land and ice, Frontiers in Environmental Science, 2, 10.3389/fenvs.2014.00041, 2014.

Stjern, C. W., Samset, B. H., Myhre, G., Forster, P. M., Hodnebrog, Ø., Andrews, T., Boucher, O., Faluvegi, G., Iversen, T., Kasoar, M., Kharin, V., Kirkevåg, A., Lamarque, J. F., Olivié, D., Richardson, T., Shawki, D., Shindell, D., Smith, C. J., Takemura, T., and Voulgarakis, A.: Rapid Adjustments Cause Weak Surface Temperature Response to Increased Black Carbon Concentrations, Journal of Geophysical Research: Atmospheres, 122, 11,462-411,481, doi:10.1002/2017JD027326, 2017.

Tang, T., Shindell, D., Samset, B. H., Boucher, O., Forster, P., Hodnebrog, Ø., Myhre, G., Sillman, S., Voulgarakis, A., Aalbergsjø, S. G., and Stjern, C. W.: Contribution of Black Carbon Aerosol to Drying of the Mediterranean, Submitted to Journal of Geophysical Research - Atmosphere, 2017.

Twomey, S.: Pollution and the planetary albedo, Atm. Env., 8, 1251-1256, doi:10.1016/0004-6981(74)90004-3, 1974.

Vautard, R., Gobiet, A., Sobolowski, S., Kjellström, E., Stegehuis, A., Watkiss, P., Mendlik, T., Landgren, O., Nikulin, G., Teichmann, C., and Jacob, D.: The European climate under a 2 °C global warming, Environmental Research Letters, 9, 034006, 10.1088/1748-9326/9/3/034006, 2014.

Vinnarasi, R., Dhanya, C. T., Chakravorty, A., and AghaKouchak, A.: Unravelling Diurnal Asymmetry of Surface Temperature in Different Climate Zones, Scientific Reports, 7, 7350, 10.1038/s41598-017-07627-5, 2017.

Vose, R. S., Easterling, D. R., and Gleason, B.: Maximum and minimum temperature trends for the globe: An update through 2004, Geophysical Research Letters, 32, 10.1029/2005gl024379, 2005.

Wilcox, L. J., Liu, Z., Samset, B. H., Hawkins, E., Lund, M. T., Nordling, K., Undorf, S., Bollasina, M., Ekman, A. M. L., Krishnan, S., Merikanto, J., and Turner, A. G.: Accelerated increases in global and Asian summer monsoon precipitation from future aerosol reductions, Atmos. Chem. Phys. Discuss., 2020, 1-30, 10.5194/acp-2019-1188, 2020.

Zhou, L., Dickinson, R. E., Tian, Y., Vose, R. S., and Dai, Y.: Impact of vegetation removal and soil aridation on diurnal temperature range in a semiarid region: Application to the Sahel, Proceedings of the National Academy of Sciences, 104, 17937-17942, 10.1073/pnas.0700290104, 2007.

https://doi.org/10.5194/acp-2020-192
Preprint. Discussion started: 4 May 2020


Atmospheric Chemistry and Physics Discussions

490

495

500

Tables and Figures

505

Table 1: Overview of models and experiments

Experiments		
BASE	Present-day conditions, with solar constant and CO_2 emissions for year 2000 (Lamarque et al., 2010). Five models ran the aerosol simulations in concentration-based mode, where BC or SO_4 concentrations were fixed at the monthly multi-model mean present-day concentrations from AeroCom Phase II (Myhre et al., 2013; Samset et al., 2013). The remaining models (indicated below) ran emission-based simulations where the BASE simulation used present-day emissions of BC or SO_4.	
CO2x2	A global instantaneous doubling of the BASE CO_2 emissions.	
BCx10	A global instantaneous tenfold increase in the BASE BC concentrations (for the concentration-based models) or emissions (for the emission-based models).	
SO4x5	Like BCx10, only for SO_4. For models doing emission-based perturbations, SO_2 (not SO_4) was perturbed.	
Models	*Aerosol simulation type*	*No. of lon x lat x lev grid cells*
CanESM2	Emission-based	128 x 68 x 22
NCAR-CESM1-CAM4	Concentration-based	144 x 96 x 17
NCAR-CESM1-CAM5	Emission-based	144 x 96 x 17
GISS-E2-R	Concentration-based	144 x 90 x 40
HadGEM2	Emission-based	192 x 144 x 17
HadGEM3	Concentration-based	192 x 144 x 17
IPSL-CM5A	Concentration-based	96 x 96 x 39
NorESM1	Concentration-based	144 x 96 x 26
MIROC-SPRINTARS	Emission-based	256 x 128 x 40

510

https://doi.org/10.5194/acp-2020-192
Preprint. Discussion started: 4 May 2020

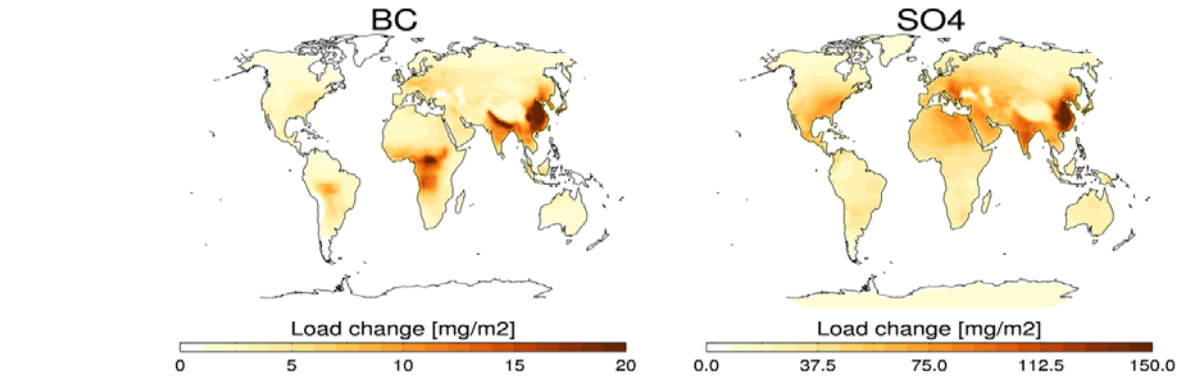

Figure 1: Geographical distribution of baseline concentrations of BC and SO4, respectively.

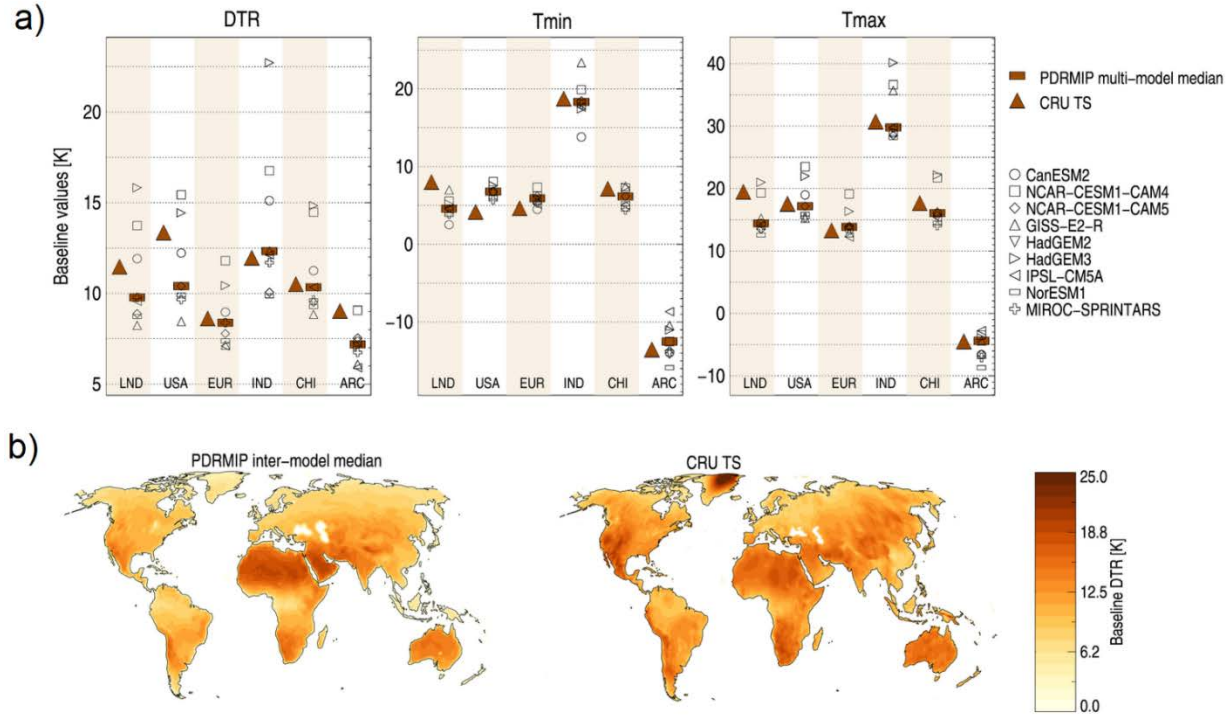

Figure 2: a) Comparison of baseline (year 2000, years 51-100 of 100-year fully coupled simulations) PDRMIP and CRU TS (mean of years 1991-2010) DTR, Tmin and Tmax. For PDRMIP, single models are shown as open symbols and multi-model median as a filled horizontal bar. Note that as HadGEM2 has a preindustrial baseline in the PDRMIP simulations (Samset et al., 2016) we have omitted this model here. b) Geographical distribution of DTR for the same years, for the PDRMIP inter-model median and for CRU.

https://doi.org/10.5194/acp-2020-192
Preprint. Discussion started: 4 May 2020

Atmospheric Chemistry and Physics Discussions

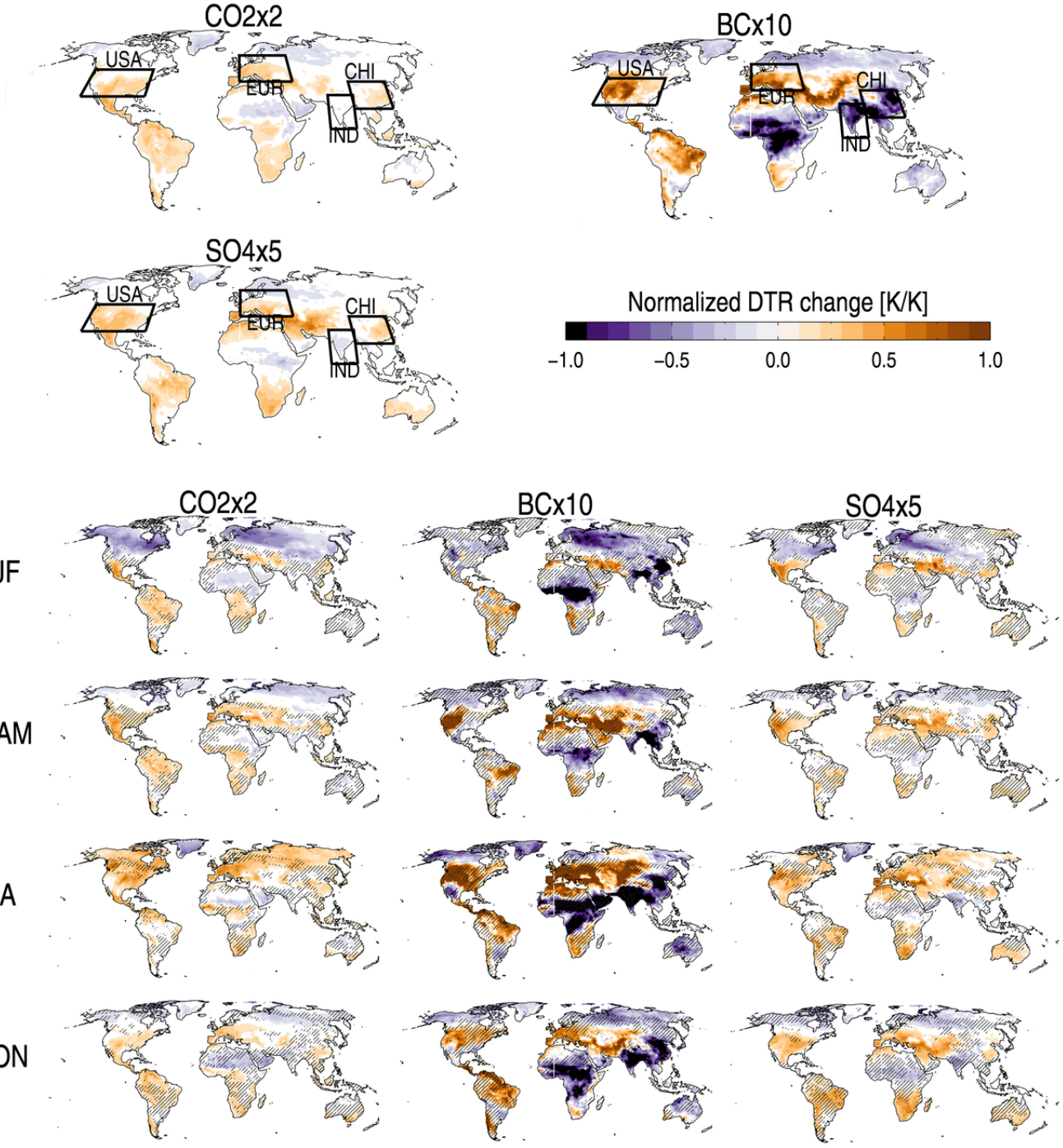

Figure 3: Multi-model median change in DTR, normalized by the global mean temperature change [K/K], for the three experiments. Large upper maps show annual mean changes, while smaller maps show seasonal changes. Hatching indicates areas where less than 75% of the models agree on the sign of the change. Annual maps include indications of the focus regions of this study. The region called "LND" throughout the manuscript is the average of all land regions on the globe.

https://doi.org/10.5194/acp-2020-192
Preprint. Discussion started: 4 May 2020

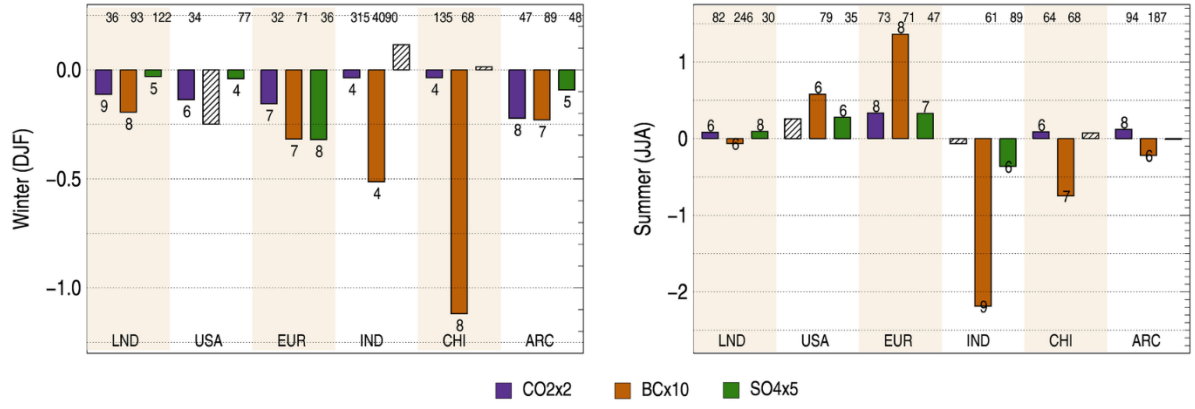

Figure 4: Multi-model median change in DTR for the different drivers and seasons, normalized by the global mean temperature change [K/K]. Cases for which 80 % of models with data have DTR changes of the same sign are marked with colors, whereas hatched bars indicate larger model disagreement. The numbers associated with the colored bars shows the number of models for which the change is statistically significant (Student's t-test p-value of less than 0.05). The coefficient of variation [std.dev/mean, %] is shown as numbers on the top.

https://doi.org/10.5194/acp-2020-192
Preprint. Discussion started: 4 May 2020

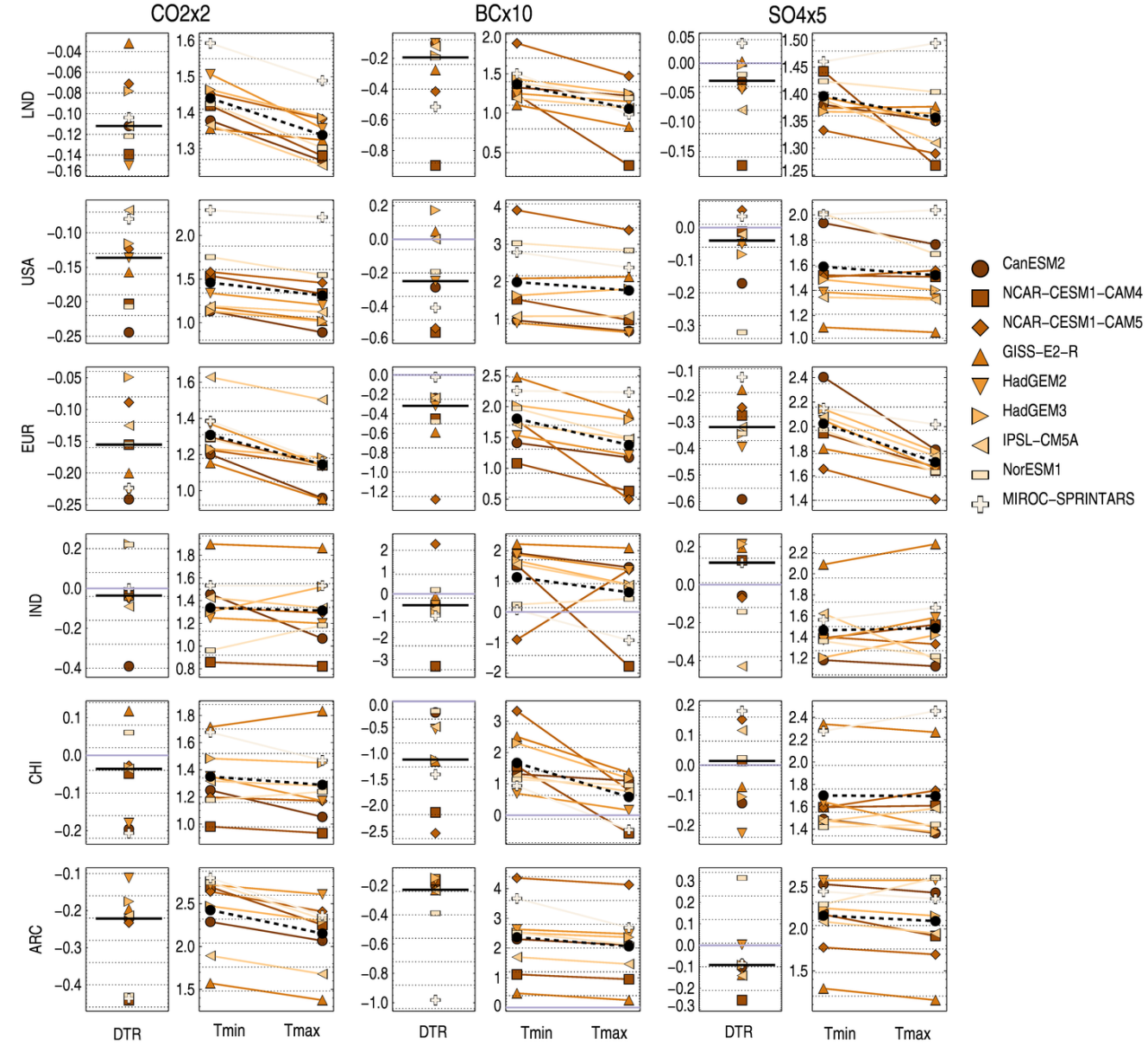

Figure 5: Regional wintertime changes in DTR, Tmin and Tmax for the three cases (columns) and six regions (rows). Black horizontal line and squares shows the multi-model median changes.

https://doi.org/10.5194/acp-2020-192
Preprint. Discussion started: 4 May 2020

Atmospheric Chemistry and Physics Discussions

565

570

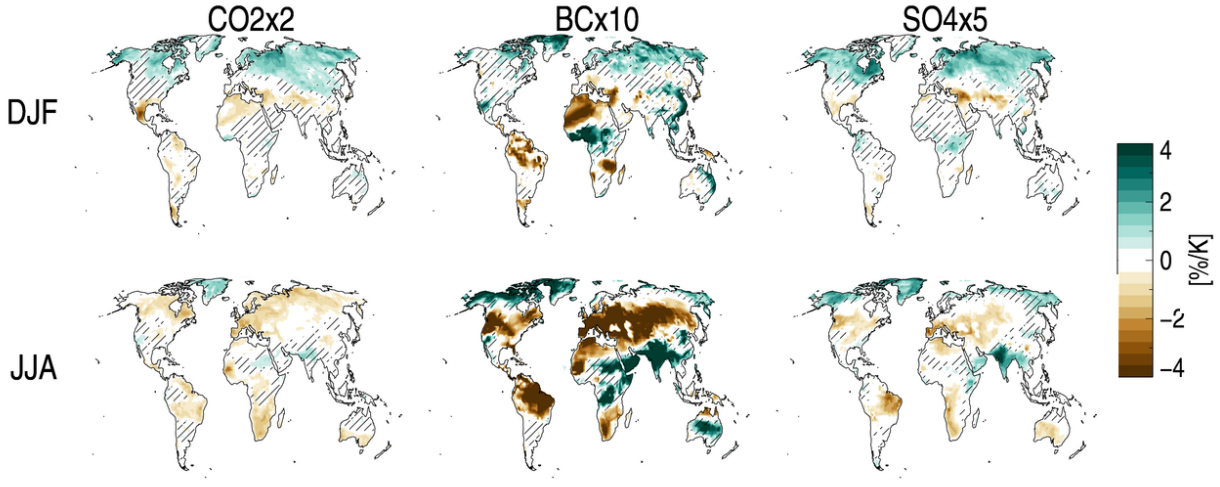

575

Figure 6: Multi-model median seasonal cloud cover change for the three drivers, normalized by the global annual mean temperature change. Hatching indicates that less than 75% of the models agree on the sign of the change.

580

https://doi.org/10.5194/acp-2020-192
Preprint. Discussion started: 4 May 2020

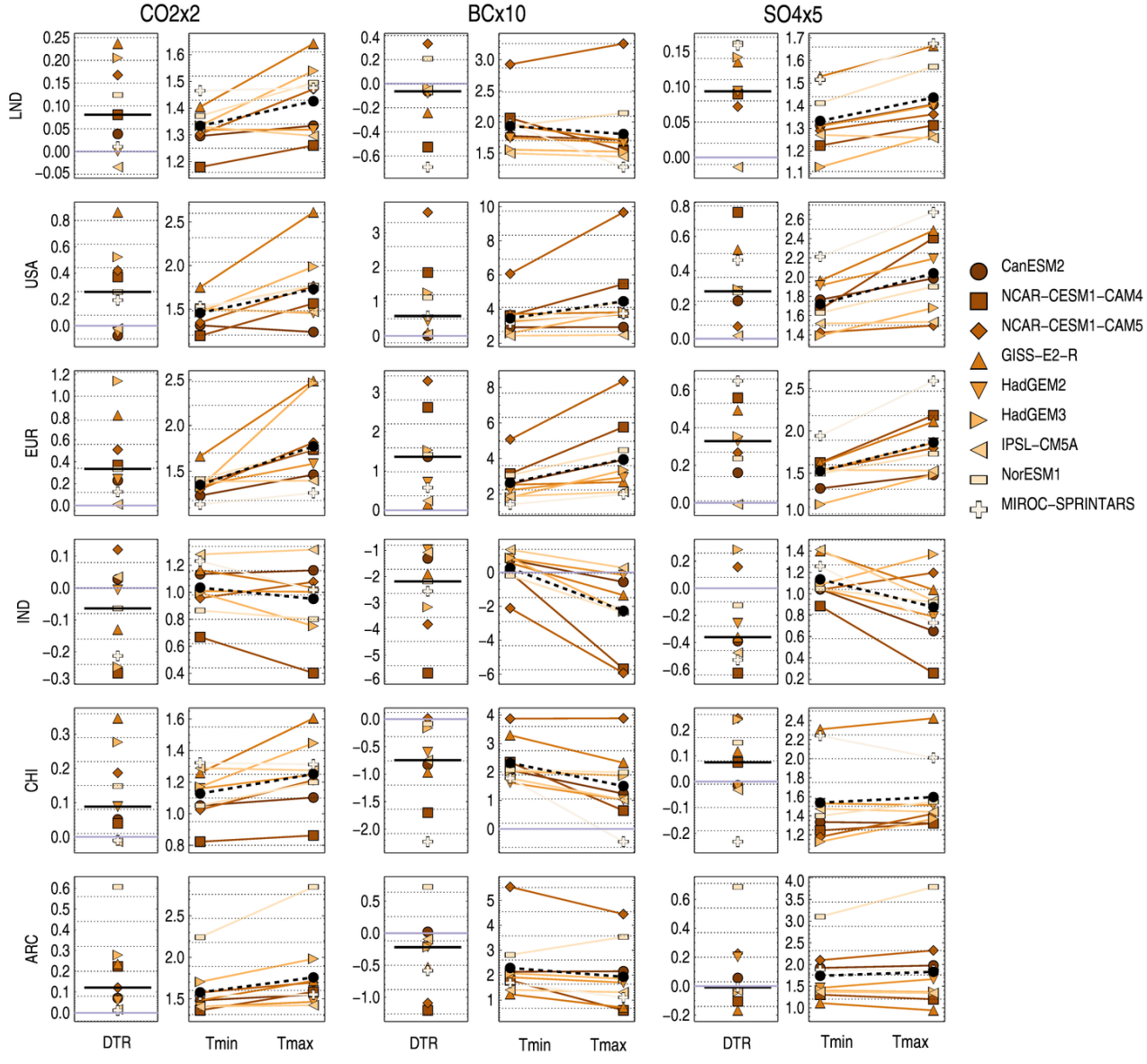

Figure 7: Regional summertime changes in DTR, Tmin and Tmax for the three cases (columns) and six regions (rows). Black horizontal line and squares shows the multi-model median changes.

https://doi.org/10.5194/acp-2020-192
Preprint. Discussion started: 4 May 2020

Atmospheric Chemistry and Physics Discussions

595

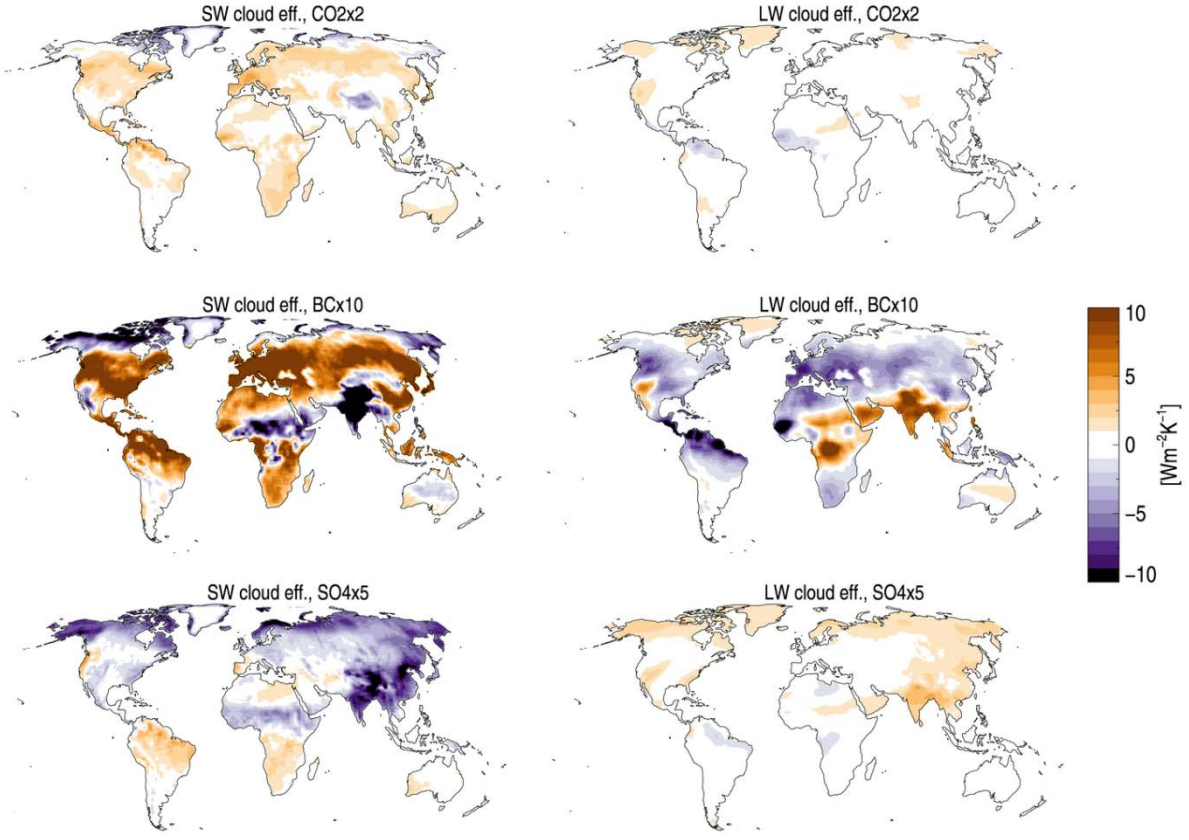

Figure 8: Multi-model median change in short-wave (SW) and long-wave (LW) cloud radiative effects [Wm^{-2}] for the JJA months, for the BCx10 experiment. See supplementary figures for maps of all seasons and experiments.

600